Supplementary Information

Synergistic enhancement of chemical looping CO_2 splitting and biomass cascade utilization using cyclic stabilized $Ca_2Fe_2O_5$ aerogel

Zhao Sun [ab], Xiaodong Wu [b], Christopher K. Russell [c], M. Darby Dyar [d], Elizabeth C. Sklute [d], Sam Toan [b], Maohong Fan [, b], Lunbo Duan [a], Wenguo Xiang [*, a]*

[a] *Key Laboratory of Energy Thermal Conversion and Control of Ministry of Education, School of Energy and Environment, Southeast University, Nanjing 210096, China*

[b] *Departments of Chemical and Petroleum Engineering, University of Wyoming, Laramie, WY 82071, USA*

[c] *Department of Civil and Environmental Engineering, Stanford University, Stanford, CA 94305, USA*

[d] *Mount Holyoke College, Department of Earth & Environment, South Hadley, MA 01075, USA*

**Corresponding author: Wenguo Xiang*

E-mail address: wgxiang@seu.edu.cn

1. Calcium ferrite aerogel preparation

When calcium nitrate tetrahydrate and iron nitrate nonahydrate were dissolved in the deionized water, reversible hydrolysis occurred. Iron and calcium hydrates are the main ions in solution. Their formation reactions are shown below:

$$Fe^{3+} + 6H_2O \rightarrow \left[Fe(H_2O)_6\right]^{3+} \quad \text{(R1)}$$

$$Ca^{2+} + 7H_2O \rightarrow \left[Ca(H_2O)_7\right]^{2+} \quad \text{(R2)}$$

It is speculated that the added propylene oxide (PA) is easily protonated due to the acidity of the iron hydrate, followed by an irreversible ring opening reaction. When calcium chloride and iron chloride are used as precursors, chloride ion is a better nucleophile than water, thus the following reactions occur:

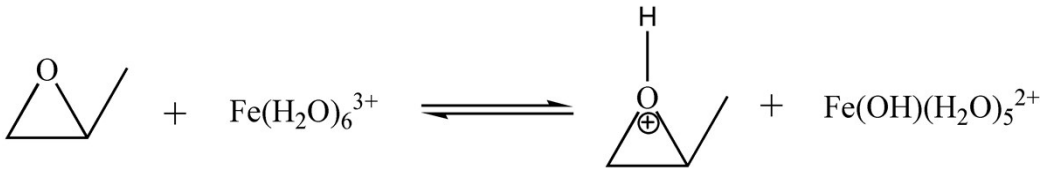

(R3)

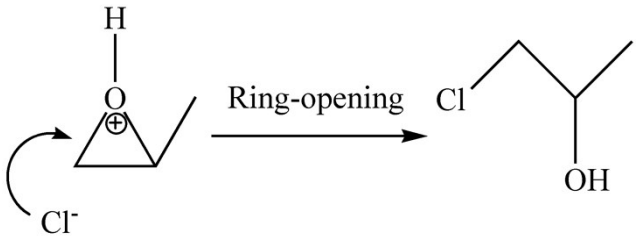

(R4)

As can be seen from (R4), no proton is produced through the ring-opening reaction of PO. Consumption of the proton leads to an increase of pH, thereby promoting the Ca-Fe gel formation. Thus, the gelation process becomes easier if calcium chloride and iron chloride are used as the precursors. However, chloride ions are prone bind tightly with Ca^{2+}, which is difficult to remove during calcination, even at temperatures above 1000 °C. Chloride ion's existence during preparation inhibits $Ca_2Fe_2O_5$ aerogel formation; thus, iron nitrate and calcium nitrate were used as the precursors.

Unfortunately, a brown-red precipitate will be generated if only PO is added. This is because 3D cross-linking is easy to be built for polyvalent metal ions such as Zr^{4+}, Cr^{3+}, Fe^{3+}, Ce^{4+}, Ti^{4+}. But this cross-link is much harder for bivalent metal ions (e.g. Cu^{2+}, Ca^{2+}, Ni^{2+}, and Zn^{2+}, etc.) to form. The presence of Ca^{2+} reduces the strength of the 3d cross-link structure, resulting in the failure of Fe-Ca composite gelation. To solve the problem, PAA was introduced to act as a

nucleophile. The synergistic effect of PAA with PO, enhances the structural strength caused by Ca^{2+} by promoting 3D cross-linking of the Ca-Fe chains. Possible reactions with the addition of PAA and PO are shown as follows:

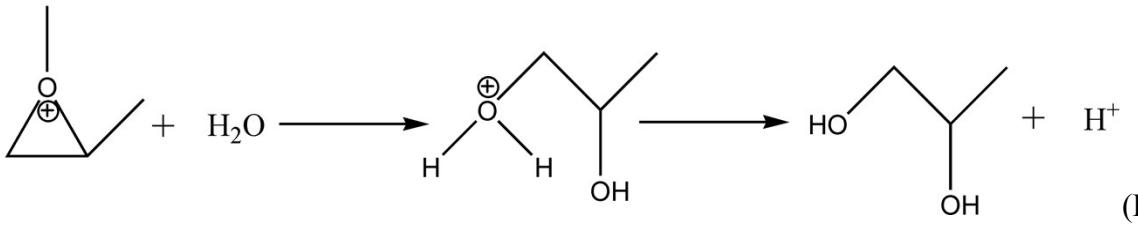

(R5)

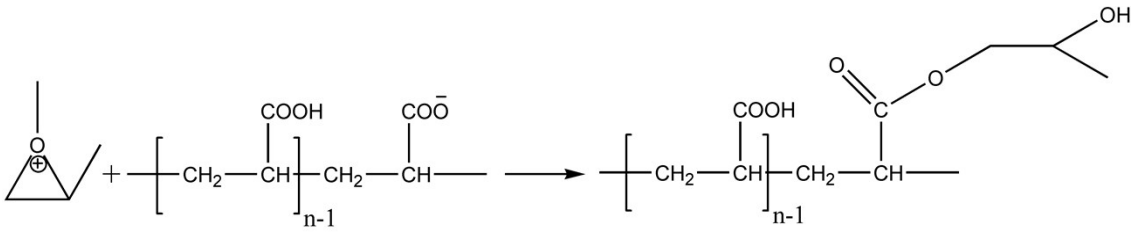

(R6)

2. *Experimental setup*

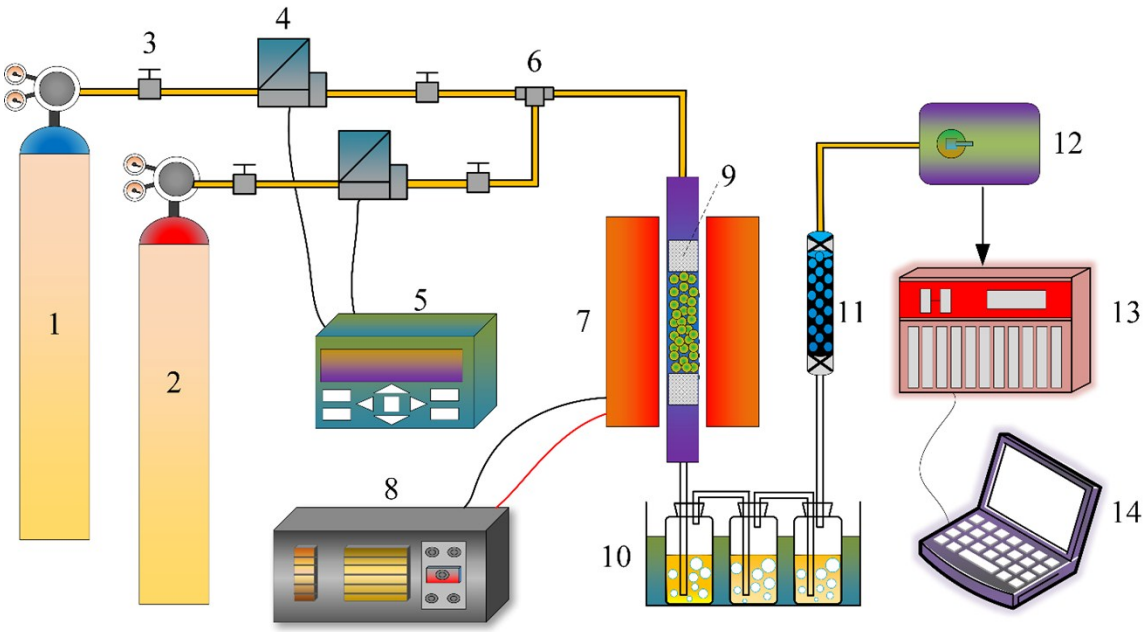

Fig. S1 Schematic diagram of fixed bed CO_2 reduction to CO system. 1) N_2 cylinder; 2) CO_2 cylinder; 3) valve; 4) mass flow meter, Parker 201, 0-100 mL/min; 5) mass flow controller, Parker CM-400; 6) three-way valve; 7) fixed bed furnace and quartz reactor, inner diameter of 1.2 cm, length of 550.0 mm; 8) temperature controller of furnace; 9) quartz wool; 10) ice bath; 11) moisture trap with dried $CaSO_4$ inside; 12) gas bags; 13) gas chromatograph, Inficon micro GC 3000; 14) computer.

3. Calculation methods

The syngas (H_2, CH_4, CO, and CO_2) concentrations were calculated as follows:

$$C_{H_2} = \frac{\mathrm{C}_{H_2,GC}}{\mathrm{C}_{H_2,GC} + C_{CH_4,GC} + C_{CO,GC} + C_{CO_2,GC}} \quad \text{(E 1)}$$

$$C_{CH_4} = \frac{C_{CH_4,GC}}{\mathrm{C}_{H_2,GC} + C_{CH_4,GC} + C_{CO,GC} + C_{CO_2,GC}} \quad \text{(E 2)}$$

$$C_{CO} = \frac{C_{CO,GC}}{\mathrm{C}_{H_2,GC} + C_{CH_4,GC} + C_{CO,GC} + C_{CO_2,GC}} \quad \text{(E 3)}$$

$$C_{CO_2} = \frac{C_{CO_2,GC}}{\mathrm{C}_{H_2,GC} + C_{CH_4,GC} + C_{CO,GC} + C_{CO_2,GC}} \quad \text{(E 4)}$$

where $\mathrm{C}_{H_2}, C_{CH_4}, C_{CO}, C_{CO_2}$ represent the calculated syngas concentrations of H_2, CH_4, CO, and CO_2, respectively. $C_{H_2,GC}, C_{CH_4,GC}, C_{CO.GC}, C_{CO_2.GC}, and\ C_{C_2-C_4,GC}$ accordingly denote the concentrations of H_2, CH_4, CO, CO_2, and C_2-C_4 detected by GC. The produced CO gas during CO_2 reduction stage is collected using gas bags at every 30 minutes per bag. The total gas yields $\mathrm{Y}_{\text{total, out}}$ for one gas bag is calculated as:

$$\mathrm{Y}_{\text{total, out}} = \frac{\mathrm{YR}_{\mathrm{N}_2,in} \times \mathrm{T}}{C_{\mathrm{N}_2,GC}} \quad \text{(E 5)}$$

where $\mathrm{Y}_{\text{total, out}}$ denotes the total gas yields from the gas sampling bag (Sigma 2L Tedlar PVDF), $\mathrm{YR}_{\mathrm{N}_2,in}$ is the flow rate of the inlet N_2, T is the N_2 flow time for each gas bag collection, and

$C_{N_2,GC}$ represents the N_2 concentration of the gas bag calculated by GC. The outlet CO yields $Y_{CO,out}$ for one gas bag is calculated in the way of:

$$Y_{CO,out} = Y_{total,out} \times C_{CO,GC} \quad \text{(E 7)}$$

The cumulative CO yield is the sum of CO obtained with every 30 minutes:

$$Y_{sum,CO,out} = \sum_{1}^{n} Y_{i,CO,out} \ (n = 1,2,3,4,5,6) \quad \text{(E 8)}$$

where $Y_{i,CO,out}$ is the CO collected with No. i gas bag and $Y_{sum,CO,out}$ represents the cumulative CO yield.

4. Experimental Results

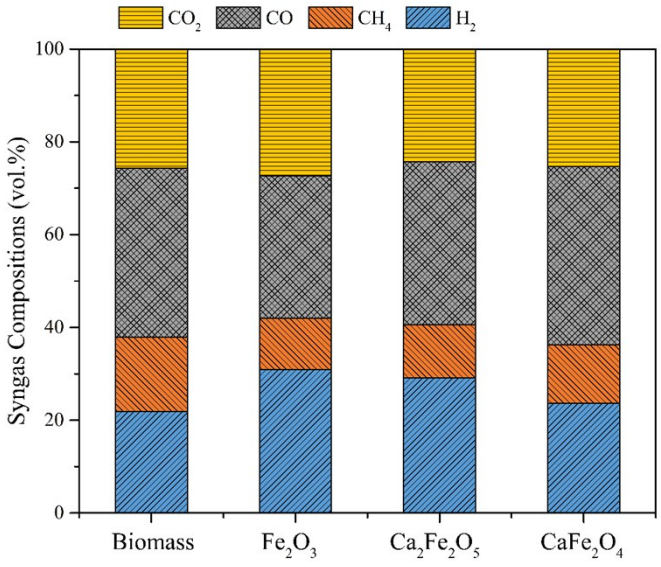

Fig. S2 Syngas compositions during catalytic fast biomass pyrolysis for Fe^{3+} reduction stage.

Number	Name	C number	Peak area (%)
1	Acetic anhydride	4	6.974
2	Butanedial	4	3.414
3	Propanoic acid, 2-methyl-, methyl ester	4	5.989
4	Furfural	5	9.297
5	2-Pentanone, 4-hydroxy-4-methyl-	6	3.255
6	2-Hexanone, 6-hydroxy-	6	3.674
7	2-Hexanone, 4-methyl-	7	5.111
8	2-Cyclopenten-1-one, 2-hydroxy-	5	4.867
9	2-Methyliminoperhydro-1,3-oxazine	5	3.872
10	2-Cyclopenten-1-one, 2-hydroxy-3-methyl-	6	3.293
11	Phenol, 2-methoxy-	7	8.531
12	Heptanal	7	4.376
13	Phenol, 2-methoxy-4-methyl-	8	13.184
14	Phenol, 4-ethyl-2-methoxy-	9	3.368
15	2-Methoxy-4-vinylphenol	9	10.179
16	Phenol, 2-methoxy-4-(1-propenyl)-	10	10.616

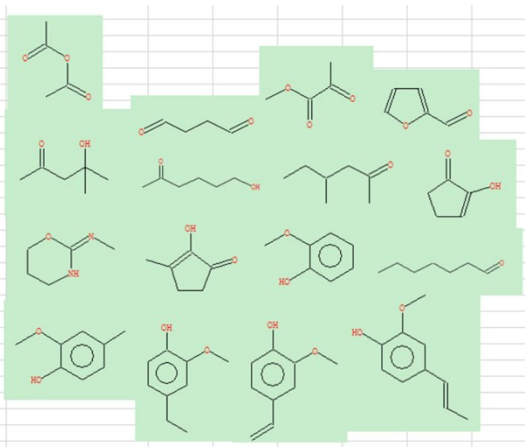

Bio-oil components from biomass fast pyrolysis

Number	Name	C number	Peak area (%)
1	Benzyl methyl ketone	9	6.18
2	Butanedial	4	2.287
3	Propanoic acid, 2-oxo-, methyl ester	4	4.42
4	Furfural	5	10.241
5	2-Pentanone, 4-hydroxy-4-methyl-	6	3.235
6	5-Hexen-2-one	6	3.455
7	2-Heptanone	7	4.918
8	2-Cyclopenten-1-one, 2-hydroxy-	5	5.199
9	2-Furancarboxaldehyde, 5-methyl-	6	4.068
10	Phenol	6	3.137
11	2-Methyliminoperhydro-1,3-oxazine	5	3.363
12	2-Cyclopenten-1-one, 2-hydroxy-3-methyl-	6	4.168
13	Phenol, 3-methyl-	6	3.999
14	Phenol, 2-methoxy-	7	6.47
15	4-Methyl-2-oxopentanenitrile	5	6.042
16	Phenol, 2-methoxy-4-methyl-	8	10.271
17	2-Methoxy-4-vinylphenol	9	8.958
18	Phenol, 2-methoxy-4-(1-propenyl)-	10	9.588

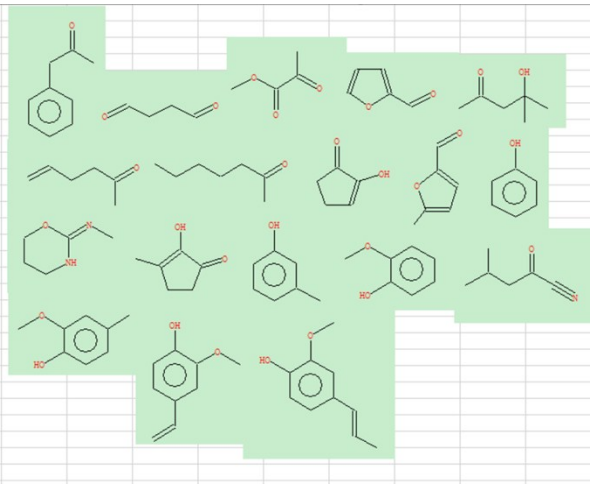

Bio-oil components from biomass fast pyrolysis with Fe_2O_3 addition

Number	Name	C number	Peak area (%)
1	Benzyl methyl ketone	9	6.249
2	Butanedial	4	2.542
3	Propanoic acid, 2-oxo-, methyl ester	4	4.32
4	Furfural	5	7.692
5	2-Pentanone, 4-hydroxy-4-methyl-	6	2.552
6	2,4-H2xadien-1-ol	6	1.934
7	p-Xylene	8	3.725
8	2-Hexanone, 4-methyl-	7	3.275
9	2-Cyclopenten-1-one, 2-methyl-	6	1.438
10	2(5H)-Furanone	4	1.731
11	2-Cyclopenten-1-one, 2-hydroxy-	5	4.116
12	2-Furancarboxaldehyde, 5-methyl-	6	3.012
13	Phenol	6	2.242
14	2-Methyliminoperhydro-1,3-oxazine	5	2.079
15	2-Cyclopenten-1-one, 2-hydroxy-3-methyl-	6	4.489
16	Phenol, 3-methyl-	7	3.306
17	Phenol, 2-methoxy-	7	6.661
18	Heptanal	7	5.285
19	Phenol, 2-methoxy-4-methyl-	8	9.584
20	Phenol, 4-ethyl-2-methoxy-	9	3.079
21	2-Methoxy-4-vinylphenol	9	8.763
22	Phenol, 2-methoxy-4-(1-propenyl)-	10	2.156
23	Phenol, 2-methoxy-4-(1-propenyl)-	10	9.769

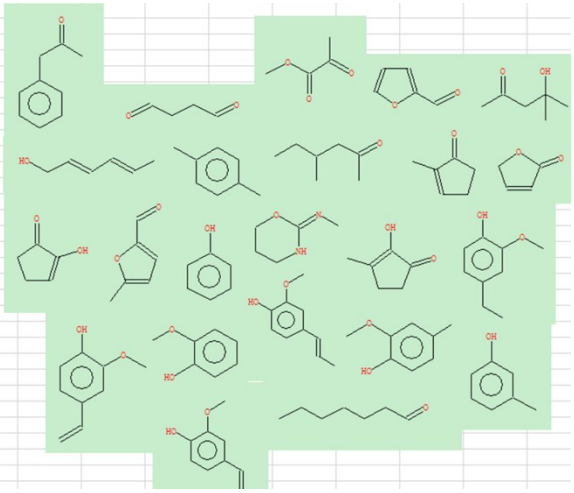

Bio-oil components from biomass fast pyrolysis with $Ca_2Fe_2O_5$ addition

Number	Name	C number	Peak area
1	Benzyl methyl ketone	9	5.487
2	Butanedial	4	2.421
3	Propanoic acid, 2-methyl-, methyl ester	4	4.333
4	Furfural	5	7.745
5	2-Pentanone, 4-hydroxy-4-methyl-	6	2.204
6	Pentane	5	3.623
7	2,4-Hexadien-1-ol	6	3.01
8	2-Heptanone	7	3.562
9	2(5H)-Furanone	4	2.174
10	2-Cyclopenten-1-one, 2-hydroxy-	5	5.104
11	2-Furancarboxaldehyde, 5-methyl-	6	1.472
12	Phenol	6	2.03
13	2-Methyliminoperhydro-1,3-oxazine	5	3.428
14	1,2-Cyclopentanedione, 3-methyl-	6	3.728
15	Phenol, 3-methyl-	7	3.254
16	Phenol, 2-methoxy-	7	6.67
17	Heptanal	7	5.711
18	Phenol, 2-methoxy-4-methyl-	8	10.76
19	Phenol, 4-ethyl-2-methoxy-	9	2.566
20	2-Methoxy-4-vinylphenol	9	9.103
21	Phenol, 2-methoxy-3-(2-propenyl)-	10	2.29
22	Phenol, 2-methoxy-4-(1-propenyl)-	10	9.324

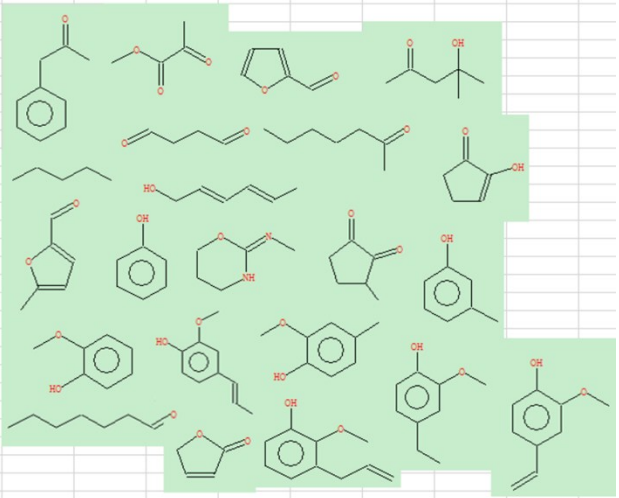

Bio-oil components from biomass fast pyrolysis with $CaFe_2O_4$ addition

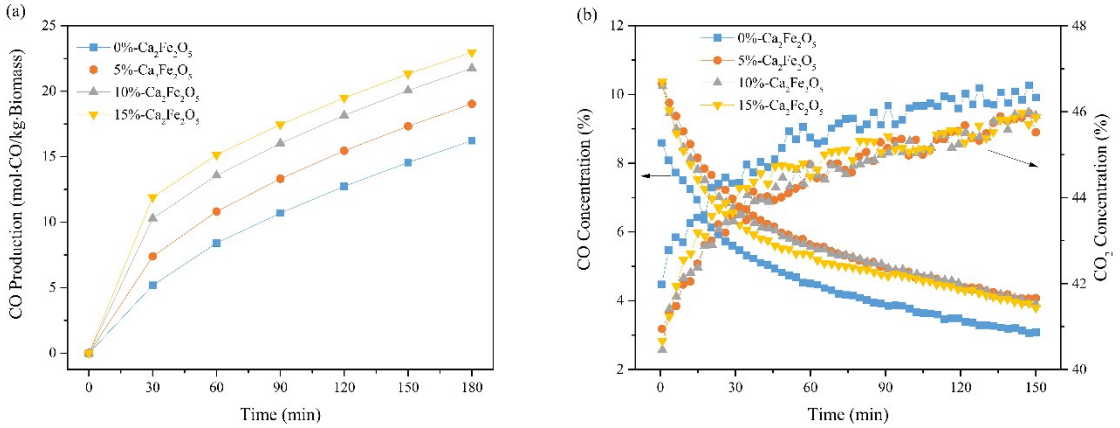

Fig. S3 a) effect of $Ca_2Fe_2O_5$ aerogel loading on the CO production; b) effect of $Ca_2Fe_2O_5$ aerogel loading on the CO production.

The effect of $Ca_2Fe_2O_5$ loading amount on cumulative CO production as well as CO and CO_2 concentration is presented in Fig. S3. Raising the $Ca_2Fe_2O_5$ loading amount promotes the CO production, mainly at the beginning of the CO_2 reduction step. The oxidation of Fe^0 generate more

CO. Subsequently, the effect of $Ca_2Fe_2O_5$ addition on CO production is relatively small, the cumulative CO production shows a trend of even growth. Moreover, similar CO concentrations can be obtained by using 5%-$Ca_2Fe_2O_5$, 10%-$Ca_2Fe_2O_5$, and 15%-$Ca_2Fe_2O_5$ aerogels, which are significantly better than the effect of no catalyst addition.

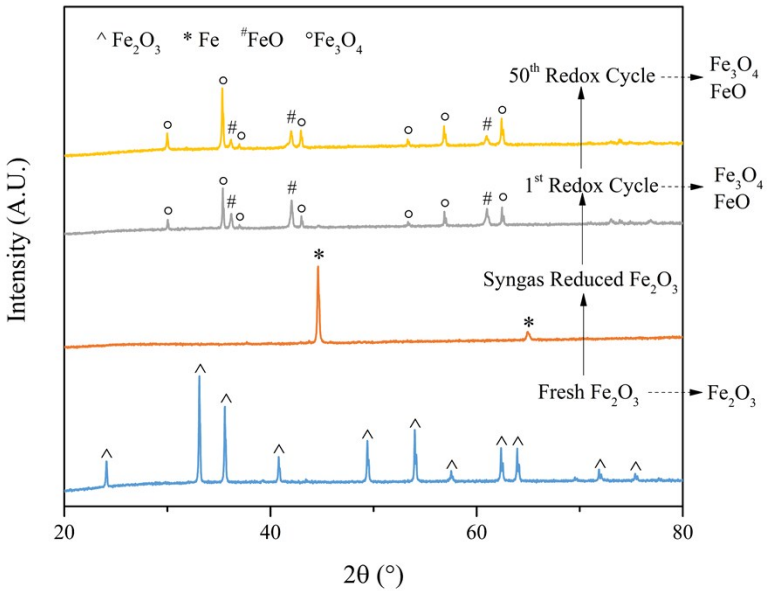

Fig. S4 XRD patterns of fresh, syngas reduced, 1st redox cycled, and 50th redox cycled Fe_2O_3.